Journal of the European Ceramic Society 19 (1998) 1769–1775

PII: S0955-2219(98)00270-2
0955-2219/99/$ - see front matter

The Thermal Shock Behaviour of Ductile Particle Toughened Alumina Composites

M. Aldridge and J. A. Yeomans*

School of Mechanical and Materials Engineering, University of Surrey, Guildford, Surrey GU2 5XH, UK

(Received 1 September 1998; accepted 7 November 1998)

Abstract

Over recent years, it has been established that the incorporation of metallic particles into a ceramic matrix can lead to enhanced fracture properties. Relatively few attempts, however, have been made to establish whether or not the improved fracture toughness typically observed in such composite systems can offer improved performance in demanding environments. The current study is concerned with the thermal shock behaviour of a ceramic matrix composite consisting of an alumina matrix containing 20 vol% of discrete iron particles. The composite material has been produced by both hot pressing and conventional sintering techniques. The hot pressed composite shows a greater resistance to thermal shock than the monolithic matrix, both in terms of the critical temperature differential and retained strength, whereas the sintered material has been found to behave as a typical low strength refractory ceramic. The calculation of thermal shock resistance parameters for the composites and the monolith has indicated possible explanations for the differences in thermal shock behaviour. © *1999 Elsevier Science Limited. All rights reserved*

Keywords: Al_2O_3 composites, thermal shock resistance, iron particulates, microstructure-final.

1 Introduction

The incorporation of a particulate metallic second phase into a ceramic matrix has been shown to increase the resistance to crack propagation in several ways. The most promising composites of this type are those with a high degree of ductile particle bridging across parting crack faces in the wake of a propagating crack (e.g. Refs.1–6). Increases in fracture toughness are also attributed to the mechanisms of crack shielding and blunting (e.g. Ref.7) and crack deflection accompanied by particle pull-out,[2,8,9] although to a lesser extent. Despite extensive work pertaining to the primary properties of ductile particle toughened ceramic matrix composites (CMCs), little is known concerning the secondary properties, in particular whether or not the improved fracture toughness alone leads to an improvement in other important properties, such as thermal shock resistance.

The theory governing the thermal shock behaviour of monolithic ceramics is well established. The classic work of Hasselman[10] showed that opposing property requirements prevail, depending on whether the material is required to be resistant to crack initiation (for which high strength and low stiffness are essential) or resistant to strength degradation following a severe thermal shock (in which case low strength and high stiffness are beneficial). Hasselman also introduced thermal shock resistance parameters (R parameters) as a means of comparing the thermal shock behaviour of ceramic materials, in terms of their physical and mechanical properties. Experimental data supporting the theoretical approach have been presented (e.g. Refs.11–13). Since the thermal shock behaviour of a ceramic material is heavily dependent on several primary mechanical properties, knowledge of the fracture toughness, fracture behaviour, fracture strength and Young's modulus of the composites is required. Therefore the scope of the current work is broadened to include the evaluation of mechanical properties relevant to thermal shock.

2 Processing and Characterisation of Composite Materials

Two alumina–iron composites were produced during the study. The first of these was hot pressed, whilst the second was pressureless sintered. Both

*To whom correspondence should be addressed. Fax: +44-(0)1483-259508.

processes involved milling the alumina and iron powders to give a blend containing 20% by volume of iron. The iron powder was common to both composites (6–9 μm powder, supplied by Johnson Matthey Ltd., Royston, UK). For the hot pressed composite, a high purity sub-micrometre alumina powder (AKP-30, supplied by Sumitomo Chemical Co. Ltd., Tokyo, Japan) was used. The blend was hot pressed in a graphite die at 1400 °C for 30 min at 25 MPa uniaxial pressure, in an atmosphere of argon, using a Clark Scientific hot press. Specimens of monolithic alumina were also prepared under identical conditions. For the sintered composite, an industrial alumina powder (supplied by Morgan Matroc Ltd., Rugby, UK) was used which contained 3% polyethyleneglycol to act as a binder. Powder compacts were cold uniaxially pressed at 20 MPa in a hardened steel die, before sintering at 1700 °C for 1 h in a tube furnace flushed continually with argon.

The microstructures of both polished and fractured specimens were examined using a Hitachi S3200N scanning electron microscope (SEM). Polished samples were prepared using conventional ceramographic techniques. Figure 1 shows typical microstructures of the hot pressed and sintered composites.

Table 1 summarises the microstructural features of the two composites in terms of grain size and metallic particle size and morphology (data for hot pressed monolithic alumina is included for comparison where appropriate). The density of the composites was measured using Archimedes' principle, and is expressed as a percentage of the maximum theoretical density (estimated using a simple rule of mixtures, assuming that no third phase has been formed).

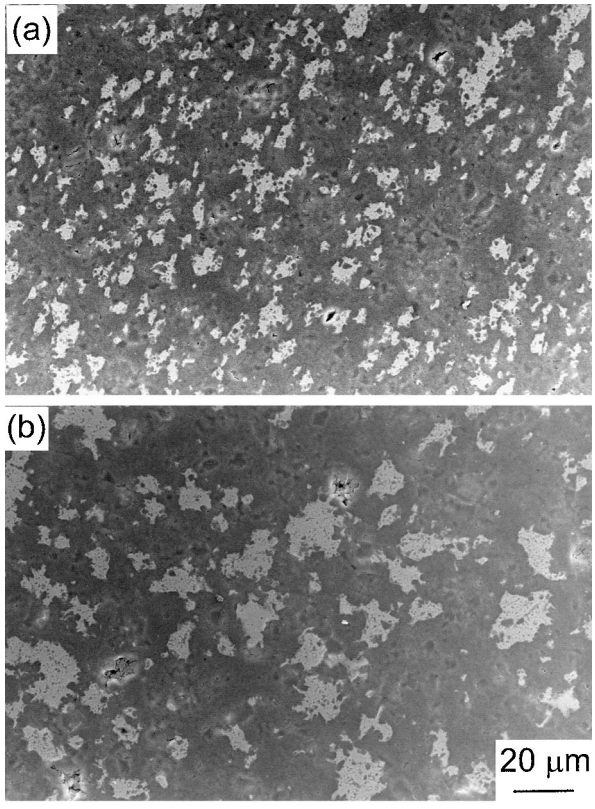

Fig. 1. Photomicrographs (secondary electron images) of (a) hot pressed and (b) sintered alumina–iron microstructures.

The microstructure of the hot pressed composite consists of an apparently random, homogeneous distribution of irregularly shaped iron particles within a dense, fine grained alumina matrix. The sintered composite shows evidence of incomplete matrix sintering (resulting in increased levels of porosity, hence the lower density). Grain growth is more prominent (due to the increased processing temperature) and the second phase particle size is increased relative to the hot pressed material. However, the sintered composite does show a homogeneous distribution of discrete, irregularly shaped metallic particles.

3 Evaluation of Mechanical Properties

3.1 Flexure strength

The flexure strength of the two composites was determined using a conventional three point loading fixture, following ASTM guidelines (C1161-90) as closely as possible. The sample size was $25\times2\times1{\cdot}5$ mm, with a loading span of 20 mm. The tensile faces of the bars were polished with a 3 (μm diamond final stage. The flexural strengths for the monolithic alumina, hot pressed composite and sintered composite were found to be 464, 641 and 148 MPa, respectively (at a probability of survival of 0·5 in each case). The strength of the monolithic alumina corresponds well with data reported in the literature. The substantially higher strength of the hot pressed composite is attributed to the decreased matrix grain size. It is concluded that the iron particles are significantly bonded to the matrix so as not to act as strength reducing flaws. The greatly decreased flexure strength of the sintered composite compared with both the monolith and the hot pressed composite is thought to be a consequence of the relatively high levels of porosity caused by

Table 1. Summary of the density and microstructural features of the hot pressed and sintered alumina–iron composites

	Density (% theoretical density)	*Grain size* (μm)	*Particle size* (μm)	*Particle shape*
Hot pressed alumina–iron	99·6	1·4	3·9	Irregular
Sintered alumina–iron	95·0	4·5	6·7	Irregular
Hot pressed alumina	99·9	2·1	—	—

the insufficient sintering of the matrix, the larger matrix grain size and possibly poor bonding between the iron particles and the matrix leading to the production of relatively large flaws.

3.2 Fracture toughness

The fracture toughness of an identical hot pressed alumina–iron composite was evaluated by Trusty[8], using the double cantilever beam (DCB) technique. The material was found to exhibit K_R curve behaviour, with the fracture toughness rising linearly to 6·6 MPa m$^{1/2}$ for a process zone length of 5·4 mm. In the same study, the K_R curve behaviour of the hot pressed monolith was found to be constant at 3·1 MPa m$^{1/2}$. A similar DCB technique has been used in the present study to evaluate the K_R curve behaviour of the sintered alumina–iron composite. Testing was performed within the chamber of a Cambridge Instruments S100 SEM, allowing precise measurement of crack length with increasing load, and observations of crack/particle interactions. The composite was found to exhibit pronounced K_R curve behaviour, with the fracture toughness rising linearly to 8·3 MPa m$^{1/2}$ for a crack length of 5 mm, as shown in Fig. 2. Examination of crack propagation indicated that the ceramic/metal interfacial bond strength was low, as interfacial failure was seen to occur in preference to plastic deformation of the ductile phase in the majority of cases.

3.3 Young's modulus

The Young's moduli of the two alumina-iron composites was measured using Grindosonic apparatus. The moduli were found to be 341 and 258 GPa for the hot pressed and sintered composites, respectively. Therefore a significant reduction in stiffness relative to the monolithic matrix is caused by the inclusion of the ductile particles. Similar trends have been reported for comparable systems (e.g. Ref.3). Several expressions exist which enable the estimation of the modulus of a composite material. Using the mechanics of materials approach, in which the metallic particles are approximated to discrete cubes in a continuous matrix, and taking the Young's modulus of the matrix as 380 GPa[14] and that of iron as 211 GPa, the modulus of both composites is estimated to be 344 GPa. Thus, there is excellent agreement between the calculated and experimental values for the hot pressed composite, as might be expected from other observations, i.e. low matrix porosity, relatively strong interfacial bonding.

Clearly, the sintered composite has a much lower Young's modulus than the calculated value. The effect of porosity on the modulus of the matrix material can be estimated using the formula proposed by Wachtman.[15] Taking the volume fraction of porosity in the matrix to be 0·06 (i.e. assuming that all of the porosity is in the matrix) modifies the matrix modulus to a value of 336 GPa, which results in a composite value of 310 GPa, which is still significantly higher than the measured value. If the modulus of the composite is estimated assuming that the iron particles are not bonded to the matrix and act as pores, the modulus is underestimated. It is therefore concluded that the interfacial bonding is poor, but it is not negligible, as observed during DCB tests.

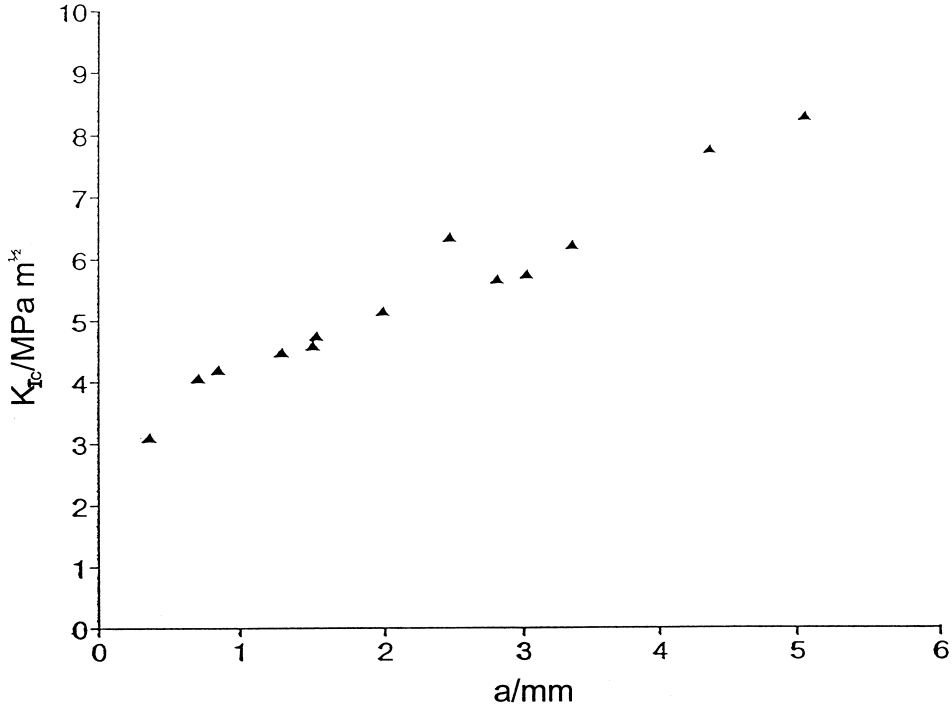

Fig. 2. K_R curve behaviour of sintered alumina–iron, measured using DCB method (data taken from two specimens).

4 Evaluation of Thermal Shock Behaviour

4.1 Retained strength

Specimens of hot pressed composite, sintered composite and hot pressed monolith were subjected to a range of temperature differentials prior to water quenching. The flexure strength was then measured as in Section 3.1. Figure 3 shows a plot of retained flexural strength versus temperature differential (ΔT) for the three materials. The curve for the monolith is similar to that reported in the literature,[11–13] showing a critical temperature differential (ΔT_c) of 200 °C and the characteristic sudden loss of strength at this point, followed by a gradual decrease for further increasing ΔT. The hot pressed composite shows a greater resistance to thermal shock, both in terms of the increased ΔT_c and the increased strength retention properties. The sintered composite behaves more like a typical refractory ceramic, showing no definitive ΔT_c, and little degradation in strength for increased ΔT.

4.2 Microscopy

Scanning electron microscopy and confocal scanning laser microscopy (CLSM) were used to examine post-shocked specimen surfaces. Samples of both hot pressed and sintered composites were subjected to a ΔT of 400 °C, then examined using a

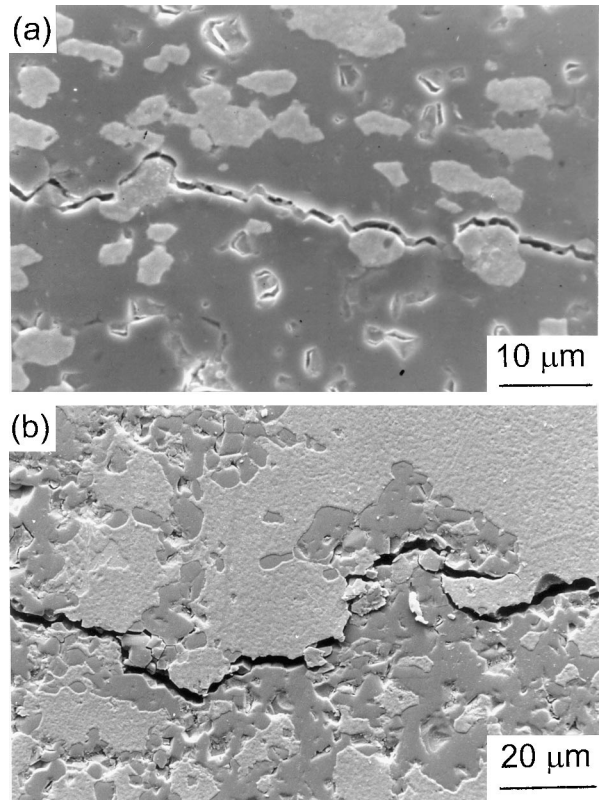

Fig. 4. Photomicrographs showing thermal shock induced cracking for $\Delta T = 400$ °C, for (a) hot pressed and (b) sintered alumina–iron composites.

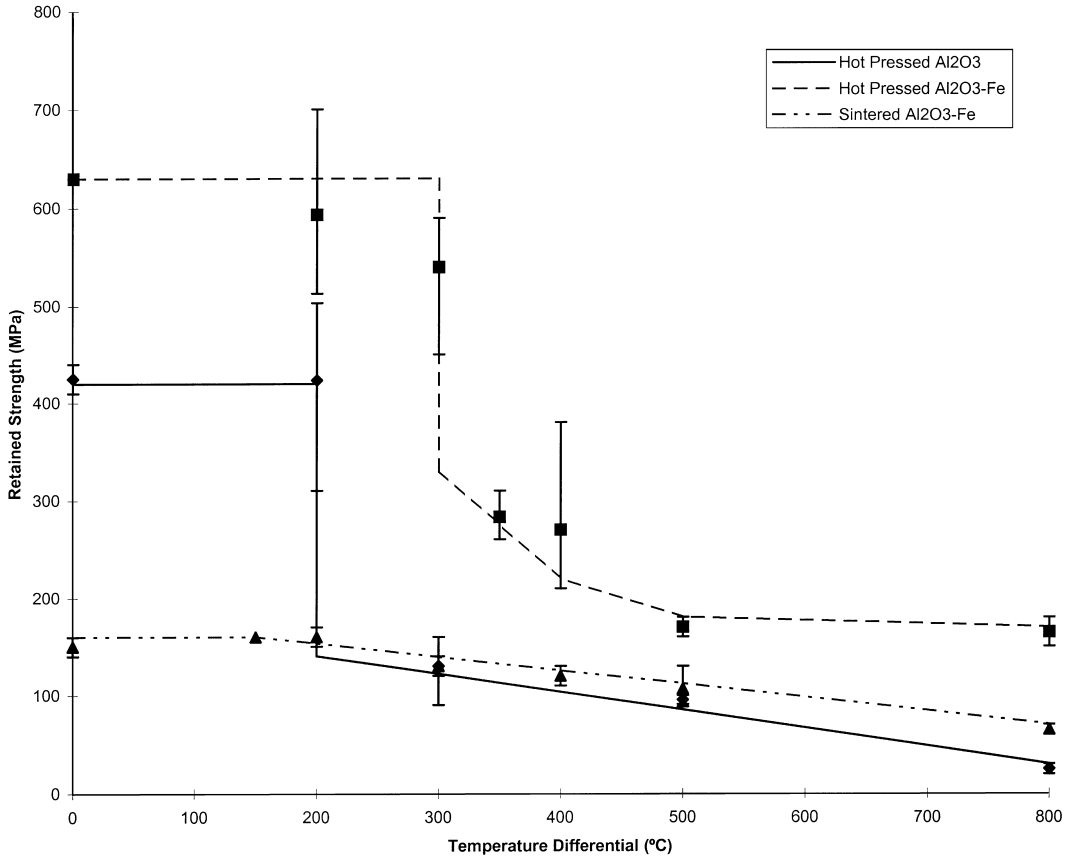

Fig. 3. Plot of retained flexure strength versus temperature differential for hot pressed alumina, hot pressed alumina–iron and sintered alumina–iron.

Cambridge Instruments S100 SEM. Cracking was observed in both cases as shown in Fig. 4. Interfacial failure was found to occur in the majority of crack/particle interactions. A CLSM (Zeiss LSM30) was used for fluorescence work. Smaller samples (2.5×2.5×2.5 mm) of hot pressed composite and monolith were subjected to a range of ΔT values, then immersed in a water-based dye in an ultrasonic bath. The dye was found to fluoresce when exposed to a laser of wavelength 446 nm. Schematic representations of the crack patterns are shown in Fig. 5. The thickness of the lines is indicative of the crack opening displacement on the specimen surface. Cracking was first observed at ΔT values of 300 and 400 °C for the hot pressed monolith and composite respectively. It is thought that the small size of the samples used for microscopy was responsible for the absence of cracking at a ΔT of 200 °C for the monolith. Crack lengths and densities were shown to be greater for the monolith than for the composite at all values of ΔT, thus supporting the data shown in Fig. 3.

4.3 Thermal shock resistance parameters

Hasselman[13] introduced thermal shock resistance parameters (R parameters) as a way of assessing the response of a ceramic material to thermal shock. R' defines the critical temperature differential at which the tensile stress imposed on the surface of the material is equal to the fracture stress, σ_f, such that

$$R' = \Delta T_c = \frac{\sigma_f(1-\nu)}{E\alpha}k$$

where ν is the Poisson's ratio, k is the thermal conductivity, E is the Young's modulus and α is the coefficient of thermal expansion. The fifth thermal shock resistance parameter, which indicates the ability of a material to resist damage following a thermal shock treatment of $\Delta T > \Delta T_c$, is given by

$$R'''' = \frac{K_{Ic}^2}{\sigma_f^2(1-\nu)}$$

where K_{Ic} is the fracture toughness. Table 2 summarises the relevant mechanical properties of the monolith, hot pressed composite and sintered composite, along with the calculated values of R' and R''''.

Whilst it is recognised that the values of Poisson's ratio, thermal conductivity and coefficient of thermal expansion for the composites are unlikely to be identical to those of monolithic alumina, it can be seen that the R parameters that have been calculated on this basis broadly support the experimental data shown in Fig. 3. Indeed, the thermal conductivity of the hot pressed composite is likely to be higher than that of either of the other two materials and to result in an increased value of R'. For the sintered material, the increase in thermal

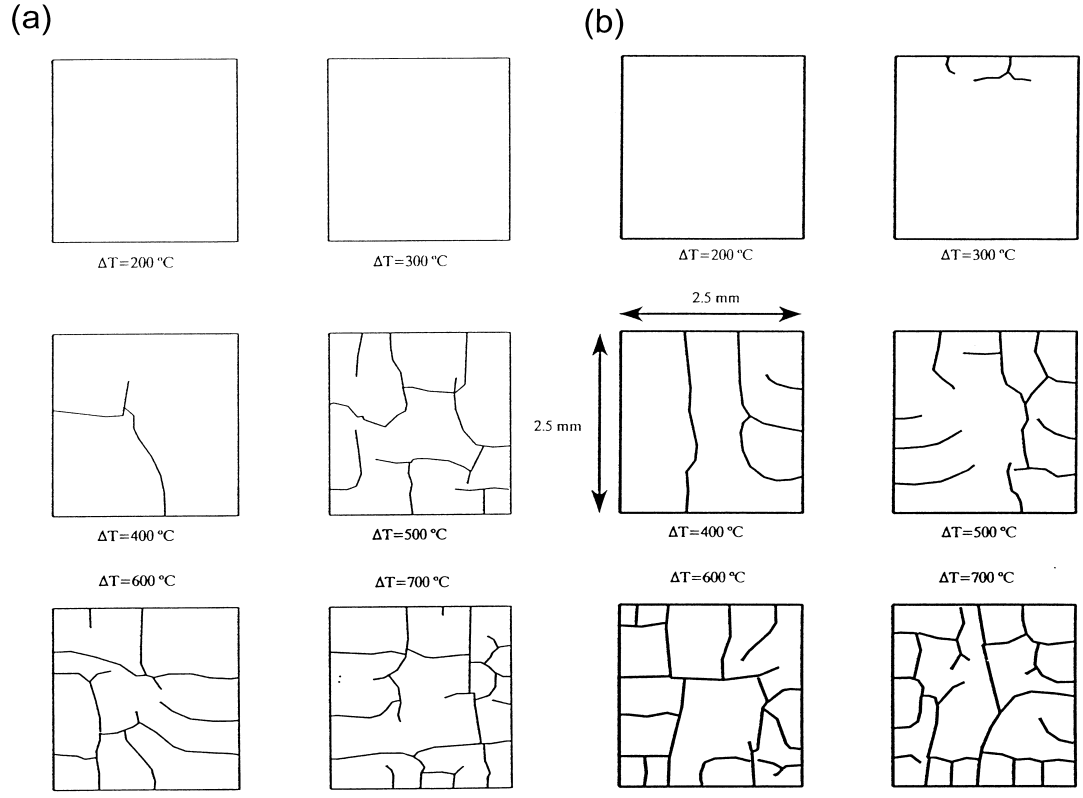

Fig. 5. Schematic representations of the cracks produced at various values of ΔT for hot pressed (a) alumina–iron composite and (b) monolithic alumina.

Table 2. Summary of relevant mechanical and thermal properties of the hot pressed monolithic alumina, hot pressed composite and sintered composite

	Hot pressed alumina	*Hot pressed alumina–iron*	*Sintered alumina–iron*
σ_f (MPa)	464	641	148
E (GPa)	380*	341	258
ν	0·22*	0·22*	0·22*
k ($W\,m^{-1}\,K^{-1}$)	20*	20*	20*
K_{Ic} ($MPa\,m^{1/2}$)	3·1	6·9	8·3
α ($\times 10^{-6}\,K^{-1}$)	7·7*	7·7*	7·7*
R' ($W\,m^{-1}$)	2474	3808	1162
R''''	57	149	4032

*Data taken from Ref.14 for monolithic alumina.

conductivity as a result of the presence of iron may be offset by the increased porosity. The larger R' calculated for the hot pressed composite indicates a higher resistance to the initiation of crack propagation under conditions of thermal shock. R' for the sintered composite is significantly lower than that for the monolith, implying that a lower critical temperature differential would be expected. This is not apparent, however, from the data shown in Fig. 3. It is possible that cracking in the sintered composite does indeed initiate for a relatively low ΔT, but that the high damage resistance of the composite results in minimal crack propagation and consequent strength degradation. Such a claim is supported by the R'''' values shown above, with the monolith showing the lowest damage resistance, and the value for the sintered composite being over 70 times greater.

Similar results were presented by Aghajanian *et al.*,[3] who fabricated a range of alumina–aluminium composites. The thermal shock resistance was found to be improved relative to the monolith for those composites showing low levels of porosity, in terms of initial room temperature strength and critical temperature differential. However, the more porous composites behaved as a refractory material, showing relatively low room temperature strength, no definite critical temperature differential and a high degree of damage tolerance.

It is unclear at this stage whether the improvement in ΔT_c of the hot pressed composite and the increased damage resistance capabilities of both the hot pressed and sintered composites are a direct consequence of the increased fracture toughness of the composites, and corresponding K_R curve behaviour. It appears that both the reduced Young's modulus and increased fracture toughness of the composites compared with the monolith contribute to the overall improvements in thermal shock behaviour observed. It is further concluded that the significant difference between the fracture strength of the two composites is responsible for the change in behaviour from a typical engineering ceramic to a refractory ceramic.

5 Conclusions

Alumina–iron composites have been fabricated using methods of hot pressing and conventional pressureless sintering. The mechanical properties of the composites relevant to thermal shock have been evaluated, including strength, toughness and stiffness. Large differences in the strengths of the sintered and hot pressed materials have been observed, and explained in terms of the differing microstructures produced by the two processing methods. The sintered composite has been shown to exhibit K_R curve behaviour similar to, although more pronounced than, that shown by the hot pressed composite.

The thermal shock behaviour of the composites has been studied experimentally, with comparisons being made with monolithic alumina. The thermal shock resistance of the hot pressed composite was found to be significantly greater than the monolith, whereas the sintered composite was found to behave as a typical low strength refractory ceramic. The calculation of thermal shock resistance parameters has supported the experimental data obtained.

Acknowledgements

One of the authors (M. A.) is grateful to the Engineering and Physical Sciences Research Council for the provision of funding. The authors wish to thank Morgan Matroc for the provision of materials and Professor Rawlings of Imperial College of Science, Technology and Medicine for the provision of the Grindosonic test data.

References

1. Hing, P. and Groves, G. W., The strength and fracture toughness of polycrystalline magnesium oxide containing metallic particles and fibres. *J. Mat. Sci.*, 1972, **7**, 427–434.
2. Krstic, V. V., Nicholson P. S., and Hoagland, R. G., Toughening of glasses by metallic particles. *J. Am. Ceram. Soc.*, 1981, **64**(9), 499–504.
3. Flinn, B. D., Rühle, M. and Evans, A. G., Toughening in composites of Al_2O_3 reinforced with Al. *Acta Met*, 1989, **37**, 3001–3006.
4. Aghajanian, M. K., Macmillan, N. H., Kennedy, C. R., Luszcz S. J., and Roy, R., Properties and microstructure of Lanxide® Al_2O_3-Al ceramic composite materials. *J. Mat. Sci.*, 1989, **24**, 658–670.
5. Tuan, W. H. and Brook, R. J., Processing of alumina/nickel composites. *J. Am. Ceram. Soc.*, 1992, **10**, 95–100.

6. Thompson, L. R. and Raj, R., In-situ stress-strain response of small metal particles embedded in a ceramic matrix. *Acta. Met*., 1994, **42**, 2477–2485.
7. Sigl, L. S., Mataga, P. A., Dalgleish, B. J., McMeeking, R. M. and Evans, A. G., On the toughness of brittle materials reinforced with a ductile phase. *Acta. Met*., 1988, **36**, 945–953.
8. Trusty, P. A. and Yeomans, J. A., The toughening of alumina with iron: effects of iron distribution on fracture toughness. *J. Am. Ceram. Soc*., 1997, **17**, 495–504.
9. Sun, X. and Yeomans, J. A., Optimization of a ductile-particle-toughened ceramic. *J. Am. Ceram. Soc*., 1996, **79**, 2705–2717.
10. Hasselman, D. P. H., Unified theory of thermal shock fracture initiation and crack propagation in brittle ceramics. *J. Am. Ceram. Soc*., 1969, **52**, 600–604.
11. Davidge, R. W. and Tappin, G., Thermal shock and fracture in ceramics. *Trans. Brit. Ceram. Soc*., 1967, **66**, 405–422.
12. Hasselman, D. P. H., Strength behaviour of polycrystalline alumina subjected to thermal shock. *J. Am. Ceram. Soc*., 1970, **53**, 490–495.
13. Gupta, T. K., Strength degradation and crack propagation in thermally shocked Al_2O_3. *J. Am. Ceram. Soc*., 1972, **55**, 249–253.
14. Morrell, R., *Handbook of Properties of Technical & Engineering Ceramics, Part 1: An Introduction for the Engineer and Designer*. HMSO, London, 1985.
15. Wachtman, J. B., *Mechanical and Thermal Properties of Ceramics*. NBS Special Publication 303. National Bureau of Standards, Washington DC, 1969.